A Theoretical Study of ^{31}P and ^{95}Mo NMR Chemical Shifts in $M(CO)_5PR_3$ (M = Cr, Mo; R = H, CH_3, C_6H_5, F, and Cl) Based on Density Functional Theory and Gauge-Including Atomic Orbitals

Yosadara Ruiz-Morales and Tom Ziegler*

Department of Chemistry, The University of Calgary, Calgary, Alberta, Canada T2N 1N4

Received: October 13, 1997; In Final Form: January 5, 1998

A theoretical study has been carried out on ^{31}P NMR chemical shifts in the phosphine-substituted metal carbonyls of the type $M(CO)_5PR_3$ (M = Cr and Mo; R = H, CH_3, C_6H_5, F, and Cl) as well as the ^{95}Mo NMR chemical shift of $Mo(CO)_5P(C_6H_5)_3$ and $Mo(CO)_5PX_3$ (X = F and Cl). The study was based on density functional theory (DFT) and gauge-including atomic orbitals (GIAO). The calculated chemical shifts and the components of the chemical shift tensor are in good agreement with the available experimental data. The coordination chemical shift expressed as the difference in the isotropic shifts $\Delta\delta = \delta_{M(CO)_5PR_3} - \delta_{PR_3}$ between PR_3 as a ligand, $\delta_{M(CO)_5PR_3}$, and free PR_3, was analyzed in detail. It was shown that the paramagnetic coupling between the π orbitals of the complexed PR_3 ligand π_{PR_3} and the d_σ metal-based LUMO of the $M(CO)_5PR_3$ complex has a positive contribution to the coordination chemical shift, $\Delta\delta$, whereas the paramagnetic couplings between σ_{PR_3} and $\pi^*_{PR_3}$ as well as π_{PR_3} and $\pi^*_{PR_3}$ of the complexed ligand have a negative contributions to $\Delta\delta$ for PF_3 and PCl_3. It is the latter type of couplings that are responsible for the total negative coordination shift in the case of PCl_3. The calculated ^{95}Mo NMR chemical shifts of $Mo(CO)_5P(C_6H_5)_3$ and $Mo(CO)_5PX_3$ (X = F and Cl) are in good agreement with experiment. The major contribution comes from the paramagnetic coupling between the occupied d_π orbitals (HOMO) and the virtual d_σ orbitals (LUMO).

1. Introduction

It has in the past decade become possible to carry out calculations on NMR chemical shifts[1−4] with increasing accuracy. In this regard, the application of density functional theory (DFT) has been especially useful for compounds containing heavy elements. The use of DFT in NMR calculations has been pioneered by Malkin[5] within the "individual gauge for localized orbitals" approach (IGLO)[3a] and subsequently applied by Kaupp[6] and Bühl.[7d,e] Schreckenbach[8a,b] and Ziegler have more recently presented in a method in which the NMR shielding tensor is calculated by combining the "gauge-including atomic orbitals" (GIAO) approach[9a,b] with density functional theory (DFT) following earlier work by Seifert[9c,d] et al. A number of applications[10] have shown that the GIAO-DFT scheme is capable of reproducing experimental values for ligand chemical shifts of transition metal complexes[10a,b,e] and chemical shifts of heavy main group elements.[10c,d] The DFT-GIAO scheme has further been extended to include the frozen core approximation[11a] and the scalar relativistic two-component Pauli type Hamiltonian[11b] for relativistic calculations. The DFT-GIAO implementation makes full use of the modern features of DFT in terms of accurate exchange−correlation (XC) energy functionals and large basis sets. The DFT-GIAO method has also been implemented by Rauhut[8c] et al. and Cheeseman[8d] et al. as well as Handy[8e] et al. The DFT-GIAO method has further been used in conjunction with hybride DFT methods[12b] by Bühl[7a−c] as well as Godbout and Oldfield.[12a] Traditional ab initio methods have also been applied by Nakatsuji[3c,13] et al. to the calculation of NMR chemical shifts in compounds containing heavy elements.

We present calculations on the ^{31}P chemical shift and chemical shift components for $M(CO)_5PR_3$ (M = Cr and Mo; R = H, CH_3, C_6H_5, F, and Cl) as well as the ^{95}Mo NMR chemical shift of $Mo(CO)_5P(C_6H_5)_3$ and $Mo(CO)_5PX_3$ (X = F and Cl) based on the GIAO-DFT approach.[8a,b,11] One objective of our study has been to test the accuracy and predictive power of the GIAO-DFT method by comparing theoretical results to the well-established experimental values and results from other theoretical methods. We shall in addition try to explain how the ^{31}P chemical shift of PR_3 is changed as the molecule is complexed to a metal center. A comparison will also be made to our recent DFT-GIAO[10a,e] studies on binary carbonyl complexes in which the difference (coordination shift) in the isotropic shielding $\Delta\delta = \sigma_{CO} - \sigma_{M(CO)n}$ between free CO and CO as a ligand, $\sigma_{M(CO)n}$ was analyzed in detail. Phosphine is similar (isolobal) to CO as a ligand in that both molecules contain a σ-type orbital, two π-type orbitals and two π^*-type orbitals, see Figure 1.

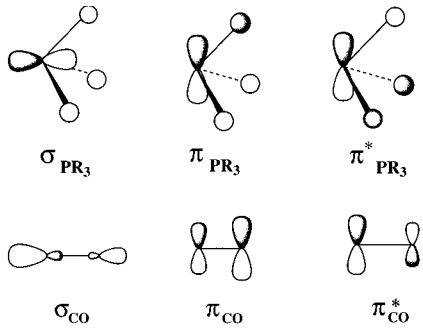

Figure 1. Frontier orbitals in PR_3 and CO.

Kaupp[6f] was the first to carry out DFT calculations on the ^{31}P coordination shifts ($\Delta\delta$) in a study on $M(CO)_5L$ [M = Cr, Mo, and W; L = PH_3, $P(CH_3)_3$, PF_3, and PCl_3] by using the sum-over-states density-functional perturbation theory (SOS-

S1089-5639(97)03308-2 CCC: $15.00
Published on Web 05/07/1998

DFPT) by Malkin[5a−c] et al. His analysis of ^{31}P shielding tensors in the free ligands in terms of canonical molecular orbitals is comparable with our findings. However, a detailed analysis of the computed trends in the metal complexes in terms of individual electronic excitations was not possible. Here, we have been able to analyze the observed coordination chemical shifts in terms of specific paramagnetic couplings between occupied and virtual orbitals. Some recent experimental solid-state ^{31}P studies on $Cr(CO)_5Ph_3$ and $Cr(CO)_4(CS)Ph_3$ makes it further possible for the first time to compare observed and calculated shift tensor components in phosphine complexes and test the DFT-GIAO method for this type of large size systems.

Wasylishen et al.[14a−d] have pioneered the recording of ^{31}P and ^{95}Mo NMR shifts in the solid state. The interpretation of ^{31}P phosphine coordination shifts in terms of the σ-donor and π-acceptor abilities of these ligands has been pioneered by Alyea[15] et al. on the basis of a number of careful experimental investigations involving $Mo(CO)_5PR_3$ complexes. Alyea[15] et al. have further included ^{95}Mo NMR in their investigation. We shall here extend our NMR shift calculations to ^{95}Mo. The field of ^{95}Mo has been reviewed by Malito.[14e]

2. Computational Details and the GIAO-DFT Method

Our implementation of the DFT-GIAO method has been described in details elsewhere.[8a−b,10] It is based on the Amsterdam density functional package ADF.[6−21] We use experimental geometries, unless otherwise stated. The exchange−correlation (XC) energy functional according to Becke[22] and Perdew[23] are employed self-consistently on top of the local density approximation (LDA).

We employ an uncontracted triple-ζ quality valence basis of Slater type atomic orbitals (STOs).[24] The valence region of the basis is extended by two sets of d (p for hydrogen) polarization functions per atomic center.

The metal center was described by an uncontracted triple-ζ STO basis set[24,25] for the outer ns, np, nd, (n+1)s, and (n+1)p orbitals extended by two sets of d polarization functions, whereas the shells of lower energy were treated by the forzen core approximation.[11a,16] The valence on phosphorus included the 1s shell and was described by an uncontracted triple-ζ STO basis augmented by two 3d and one 4f function, corresponding to basis set V of the ADF package.[21] A set of auxiliary[26] s, p, d, f, and g STO functions, centered on all nuclei, was used in order to fit the molecular density and present Coulomb and exchange potentials accurately in each SCF cycle.

The NMR shielding tensor for nucleus N can be written as[8a]

$$\sigma_{\lambda\nu} = \sigma^{\mathrm{d}}_{\lambda\nu} + \sigma^{\mathrm{p}}_{\lambda\nu} = \int \frac{\vec{r}_{\mathrm{N}} \times [\vec{J}^{\mathrm{d}}_{\nu}(\vec{r}_{\mathrm{N}}) + \vec{J}^{\mathrm{p}}_{\nu}(\vec{r}_{\mathrm{N}})]_{\lambda}}{r^3_{\mathrm{N}}} \mathrm{d}\vec{r}_{\mathrm{N}} \quad (1)$$

Here $\vec{J}^{\mathrm{d}}$ and $\vec{J}^{\mathrm{p}}$ are respectively the diamagnetic and paramagnetic current densities[8a] induced by an external magnetic field $\vec{B}_{\mathrm{o}}$. Equation 1 involves an expectation value of r_{N}^{-3} where r_{N} is the distance to the NMR nucleus. The paramagnetic current density originates primarily from a coupling between occupied Ψ_{i} and virtual orbitals Ψ_{a}, induced by the external magnetic field $\vec{B}_{\mathrm{o}}$

$$\vec{J}^{\mathrm{p}} = \sum_{s=1}^{3} \sum_{i}^{\mathrm{occ}} \sum_{a}^{\mathrm{uocc}} u^{(1,\mathrm{s})}_{ai} [\Psi_i \vec{\nabla} \Psi_a - \Psi_a \vec{\nabla} \Psi_i] B_{o,s} \quad (2)$$

The principle contribution to the coupling $u^{(1)}_{ai}$ is given by

$$u^{(1)}_{ai} \approx \propto - \frac{1}{2(\epsilon^{(0)}_i - \epsilon^{(0)}_a)} \sum_{\lambda,\nu} c^{(0)}_{\lambda a} c^{(0)}_{\nu i} \{\langle \chi_\lambda | [\vec{r}_\nu \times \vec{\nabla}]_u | \chi_\nu \rangle\}$$

$$\propto - \frac{1}{2(\epsilon^{(0)}_i - \epsilon^{(0)}_a)} \langle \Psi_a | \hat{M}|_u \Psi_i \rangle \quad (3)$$

Here $\epsilon^{(0)}$ refers to orbital energies of the unperturbed molecules without the external magnetic field. $\langle \Psi_a | \hat{M}_u | \Psi_i \rangle$ represents the first-order magnetic coupling between an occupied molecular orbital, i, and a virtual orbital, a. Within the GIAO formalism,[8a] the action of the magnetic operator $\hat{M}_u$ on Ψ_q is simply to work with $i\hat{L}^{\nu}_u$ on each atomic orbital x_ν. Here $\hat{L}^{\nu}_u$ is the u-component of the angular momentum operator with its origin at the center $\vec{R}_\nu$ on which x_ν is situated. Tabulations for $\hat{L}^{\nu}_u x_\nu$ are available in the literature.[27,28]

3. Results and Discussions

We shall now provide a discussion of how the ^{31}P shift tensor in PR_3 is modified as the PR_3 molecule is complexed to a metal center. The discussion will start with the free PR_3 ligand and continue to $(CO)_5MPR_3$ in the following sections. The coordinate systems are always chosen such that the z-axis points along the C_3-axis in the free ligand or the M−P bond vector in the $(CO)_5MPR_3$ complexes. The x-axis is placed in the C_s reflexation plane of the $(CO)_5MPR_3$ complex.

The chemical shift of a sample nuclei relative to a reference can be written with sufficient accuracy for our purpose as[29a]

$$\delta_{\mathrm{sample}} = \sigma_{\mathrm{reference}} - \sigma_{\mathrm{sample}} \quad (4a)$$

Complexation of a ligand to a metal is accompanied by changes in the chemical shifts of the ligand atoms. These effects are usually analyzed in terms of the coordination chemical shift. The coordination shift is defined as[29b]

$$\Delta\delta = \delta_{\mathrm{complex}} - \delta_{\mathrm{ligand}} \quad (4b)$$

In our discussion the shielding terminology (σ) will be employed as well. Given the opposite signs of σ (shielding) and δ (chemical shift), the coordination shift should be defined in terms of the shielding terminology as

$$\Delta\delta = \sigma_{\mathrm{ligand}} - \sigma_{\mathrm{complex}} \quad (4c)$$

Thus, the coordination shift is defined as the difference in the shielding of the free ligand and the shielding of the ligand in the complex.

4. Free PR_3

The ^{31}P NMR paramagnetic, diamagnetic, and isotropic components of the chemical shielding tensor for the free phosphines are presented in Table 1 together with the available experimental data. Experimental structures idealized to C_{3v} symmetry have been used in all calculations on the free PR_3 molecule. The components of the shielding tensors perpendicular and parallel to the C_3 axis are given as $\sigma_\perp$ and $\sigma_\parallel$, respectively. There is a good agreement between theory and experiment for PH_3, $P(CH_3)_3$, and $P(C_6H_5)_3$ with deviations of 15 ppm. The agreement is less satisfactory for PF_3 and PCl_3 with deviations up to 60 ppm.

The total shielding components $\sigma_\perp$ and $\sigma_\parallel$ are dominated by large positive diamagnetic contributions $\sigma^{\mathrm{d}}_\perp$ and $\sigma^{\mathrm{d}}_\parallel$ whereas the paramagnetic components $\sigma^{\mathrm{p}}_\perp$ and $\sigma^{\mathrm{p}}_\parallel$ are negative, and in most

TABLE 1: Experimental and Calculated Shielding Tensors[a] for Free Phosphines[a]

molecule	$\sigma_{\perp}^{d}$	$\sigma_{\perp}^{p}$	$\sigma_{\perp}$	$\sigma_{\parallel}^{d}$	$\sigma_{\parallel}^{p}$	$\sigma_{\parallel}$	σ
PH_3	965.4 (981.5)[b]	−372.2 (−368.4)[b]	593.2 (613.1)[b]	963.5 (980.0)[b]	−439.4 (−422.9)[b]	524.1 (557.1)[b]	570.2 (594.4)[b]
$P(CH_3)_3$	958.3	−559.7	398.6 (389.2)[b]	946.6	−586.0	360.6 (396.8)[b]	385.9 (391.7)[b]
PPh_3	959.5	−645.9	313.6 (319.3)[c,d]	953.6	−618.9	334.7 (370.3)[c,d]	320.6 (336.3)[c,d]
PF_3	948.5	−857.2	91.3 (162.4)[b]	938.8	−583.9	354.9 (343.4)[b]	179.2 (222.7)[b]
PCl_3	966.9	−971.8	−4.9	958.6	−811.5	147.1	45.8 (111.3)[b]

[a] All numbers are in ppm. The component $\sigma_{\perp}$ is perpendicular to C_{3v} axis, $\sigma_{\parallel}$ is parallel to C_3 axis. Superscrips p and d indicate paramagnetic and diamagnetic components, respectively. [b] Experimental numbers from ref 45. [c] Experimental numbers from ref 40. [d] Experimental numbers are in parentheses. Experimental data originally reported as chemical shift (δ) were converted to absolute shielding (σ) using the experimental data ^{31}P in 85% H_3PO_4 (aq) $\sigma_{H_3PO_4}$= 328.35 ppm (ref 45) and $\delta = \sigma_{H_3PO_4} - \sigma_{substance}$.

TABLE 2: Calculated and Experimental ^{31}P Chemical Shift Tensor Components and Isotropic Chemical Shift for Free PR_3 and $M(CO)_5PR_3$ (Values in ppm) Comparison with ^{13}C for Free CO and $Cr(CO_6)$

system	cone angle	δ_{xx}[y]	δ_{yy}[y]	δ_{zz}[y]	δ^{d}	δ^{p}	chemical shift δ (exptl)[r]
CO[c]		328.9 (317.7)[r]	328.9 (317.7)	−94.1 (−88.0)	−4.6	192.5	187.9(184.4)
$Cr(CO)_6$[c]		354.0 (353.0)	354.0 (353.0)	−86.3 (−70.0)	−12.1	219.3	207.2 (212.0)
PH_3[f]	87.0[j]	−277.7 (−284.8)[s]	−277.7 (−284.8)[s]	−208.6 (−228.8)[s]	−9.1	−245.6	−254.7[a] (−266.1)[s]
$Cr(CO)_5PH_3$[g]		−67.5	−67.5	−211.1	−12.5	−102.9	−115.4[a] (−129.6)[b]
$Mo(CO)_5PH_3$[q]		−113.1	−113.1	−210.8	−13.3	−132.4	−145.7[a] (−165.0)[d]
$P(CH_3)_3$[e]	118.0[j]	−83.1 (−60.8)[s]	−83.1 (−60.8)[s]	−45.1 (−68.4)[s]	1.3	−71.7	−70.4[a] (−63.4)[s]
$Cr(CO)_5P(CH_3)_3$[h]		45.1	45.1	−45.1	7.2	7.8	15.0[a] (6.5)[i]
$Mo(CO)_5P(CH_3)_3$[n]		6.1	6.1	−45.0	2.1	−13.0	−10.9[a] (−17.0)[d]
PPh_3[l]	145.0[j]	1.9 (9.0)[k]	1.9 (9.0)[k]	−19.2 (−42.0)[k]	−1.8	−3.3	−5.1[a] (−8.0)[k]
$Cr(CO)_5PPh_3$[m]		106.8 (127.0)[k]	94.2 (80.0)[k]	−7.4 (−42.0)[k]	1.4	63.1	64.5[a] (55.0)[k]
$Mo(CO)_5PPh_3$[o]		85.5	71.1	−7.9	0.4	50.1	50.5[a] (38.0)[d]
$Cr(CO)_4(CS)PPh_3$[k]		112.6 (101.0)[k]	106.9 (70.0)[k]	−20.2 (−37.0)[k]	1.1	65.3	66.4[a] (46.0)[k]
PF_3[v]	104.0[w]	224.2 (166.0)[s]	224.2 (166.0)[s]	−39.4 (−15.0)[s]	10.4	125.9	136.3[a] (105.7)[s]
$Cr(CO)_5PF_3$[g]		361.2	361.2	−117.3	10.4	191.4	201.7[a] (174.0)[z]
$Mo(CO)_5PF_3$[p]		312.9	312.9	−97.1	10.7	165.5	176.2[a] (147.0)[d]
PCl_3[u]	124.0[w]	320.4	320.4	168.4	−8.5	278.2	269.7[a] (217.1)[s]
$Cr(CO)_5PCl_3$[t]		340.5	340.5	−44.3	−16.2	228.5	212.3[a] (187.0)[d]
$Mo(CO)_5PCl_3$[g]		347.6	347.6	27.4	−16.0	256.9	240.9[a] (152.4)[x]

[a] Calculated absolute chemical shielding $\sigma_{H_3PO_4}$ = 315.5 ppm, $\sigma^{d}_{H_3PO_4}$ = 955.7 ppm, $\sigma^{p}_{H_3PO_4}$ = −640.2 ppm; structural data from ref 34, (exptl value: ^{31}P in 85% H_3PO_4 (aq) $\sigma_{H_3PO_4}$ = 328.35 ppm, ref 45), and $\delta = \sigma_{H_3PO_4} - \sigma_{substance}$, $\sigma^{d} = \sigma^{d}_{H_3PO_4} - \sigma^{d}_{substance}$, $\delta^{p} = \sigma^{p}_{H_3PO_4} - \sigma^{p}_{substance}$. [b] Reference 35. [c] Reference 10a. [d] Reference 1a. [e] Structural data from ref 36. [f] Structural data from ref 37. [g] Optimized structure. [h] Structural data from ref 38. [i] Reference 39. [j] Reference 33. [k] Reference 40. [l] Reference 41. [m] Reference 42. [n] Reference 43. [o] Reference 44. [p] Reference 47. [q] Optimized structure. [r] Experimental values in parantheses. The experimental data are reported with respect to ^{31}P in 85% H_3PO_4 (aq). [s] Reference 45. Experimental data originally reported as absolute shieldings (σ) were converted to chemical shifts (δ) using the experimental data ^{31}P in 85% H_3PO_4 (aq) $\sigma_{H_3PO_4}$ = 328.35 ppm (ref 45) and $\delta = \sigma_{H_3PO_4} - \sigma_{substance}$. [t] Structural data from ref 43. [u] Structural data from ref 46. [v] Reference 37. [w] Reference 14. [x] Reference 15. [y] For all the systems except for $M(CO)_5PPh_3$ and $Cr(CO)_4(CS)PPh_3$ δ_{xx} and δ_{yy} are the perpendicular components, $\delta_{\perp}$, of the chemical shift tensor and δ_{zz} is the parallel component, $\delta_{\parallel}$, of the chemical shift tensor. [z] Reference 48.

cases smaller in absolute terms, Table 1. The diamagnetic components will not contribute much to the chemical shift (relative to H_3PO_4)

$$\delta = \sigma_{H_3PO_4} - \sigma_{compound} = \delta^{d} + \delta^{p} \quad (5)$$

since the diamagnetic shielding largely comes from constant core terms that are the same in all phosphorus compound and thus cancel out in the expression for the diamagnetic shift

$$\delta^{d} = \sigma^{d}_{H_3PO_4} - \sigma^{d}_{compound} \quad (6)$$

The chemical shift is instead dominated by the paramagnetic contribution

$$\delta^{p} = \sigma^{p}_{H_3PO_4} - \sigma^{p}_{compound} \quad (7)$$

as the paramagnetic shielding σ^{p} varies considerable among phosphorus compound, Table 1. The calculated chemical shifts for the free PR_3 molecules are given in Table 2.

The leading paramagnetic contribution to $\sigma_{\perp}^{p}$ (Table 1) comes from the coupling between the occupied σ_{PR_3} HOMO, **1a**, and the virtual $\pi^*_{PR_3}$ orbitals, **1b**, of PR_3 through the matrix elements $\langle \sigma_{PR_3} | \hat{M}_s | \pi^*_{PR_3} \rangle$ ($s = x$ or y)[31]. The function $\hat{M}_x | \pi^*_{PR_3} \rangle$, **1c**[32], will have the form of a σ-type orbital, and thus overlap with the HOMO **1a**. The same type of coupling is found in the case of free CO[10a] between σ_{CO} and π^*_{CO}.

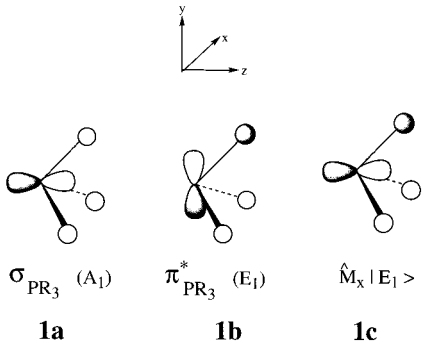

The paramagnetic shielding component $\sigma_{\perp}^{p}$ is inversely proportional to the gap between occupied and virtual orbitals, eq 3. The orbital energies of the occupied σ_{PR_3} orbitals and the virtual $\pi^*_{PR_3}$ orbitals are reported in Table 3 along with the energy gap. It is observed from Tables 1 and 3 that, in general, without considering PF_3, the smaller the energy gap the larger the paramagnetic shielding $\sigma_{\perp}^{p}$ components in absolute terms $|\sigma_{\perp}^{p}|$. PCl_3 presents the smallest energy gap and the largest value for $|\sigma_{\perp}^{p}|$. PF_3 has the largest energy gap but it does present the smallest value for $|\sigma_{\perp}^{p}|$ as expected. In this case

TABLE 3: Orbital Energies for the σ_{PR_3}-, π_{PR_3}-, and $\pi^*_{PR_3}$-Type Orbitals and Energy Gaps between σ and π^* and π and π^* Orbitals for the Free Phosphines

	orbital energy (ev)				
system	π-type orbital	σ-type orbital	π^*-type orbital	energy gap between σ and π^* orbitals (eV)	energy gap between π and π^* orbitals (eV)
PH_3	−9.603	−6.812	−0.365	6.447	9.238
$P(CH_3)_3$	−7.904	−5.000	0.615	5.615	8.519
PPh_3	−8.259	−5.571	0.308	5.879	8.567
PF_3	−14.349	−8.244	−1.676	6.568	12.673
PCl_3	−11.795	−7.288	−2.419	4.869	9.376

other factors defining $\sigma^p_\perp$ such as the magnitude of the matrix elements $\langle\Psi_a|\hat{M}_u|\Psi_i\rangle$, eq 3, and the r_N^{-3} factor in the integrant of eq 1 become important as well. There is a good agreement between theory and experiment for the perpendicular shielding component $\sigma_\perp$ in the case of PH_3, $P(CH_3)_3$, and $P(C_6H_5)_3$. The error in $\sigma_\perp$ is much larger for PF_3. We attribute the error for PF_3 and PCl_3 to an overestimation of $|\sigma^p_\perp|$.

The parallel paramagnetic shielding component $\sigma^p_\parallel$ comes from the coupling between the occupied π_{PR_3} orbitals, **2a**, and $\pi^*_{PR_3}$, **2b**, through the common lobes in $\hat{M}_z|\pi^*_{PR_3}\rangle$. For the case of free CO the paramagnetic contribution $\sigma^p_\parallel$ is zero. This is due to the fact that $\langle\pi_{y_{CO}}|\hat{M}_z|\pi^*_{x_{CO}}\rangle = 0$ because $\hat{M}_z|\pi^*_{x_{CO}}\rangle$ happens to be equal to $\pi^*_{y_{CO}}$ and $\langle\pi_{y_{CO}}|\pi^*_{y_{CO}}\rangle = 0$.

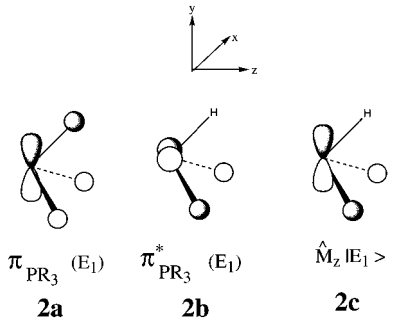

The energy gap between $\pi^*_{PR_3}$ and π_{PR_3} is smaller in PMe_3 and $P(C_6H_5)_3$ than in PH_3, Table 3, this produces a numerically larger paramagnetic $\sigma^p_\perp$ shielding in PMe_3 and $P(C_6H_5)_3$ compared to PH_3, Table 1. For the PX_3 systems $\sigma^p_\perp$ is numerically large in the case of PF_3 although it has the biggest energy gap, Table 3. Again, other factors seems to be dominating for this molecule.

Kaupp[6f] found from a set of SOS-DFPT calculations that the most important contributions to the ^{31}P chemical shift of free PR_3 are due to paramagnetic couplings between the occupied P−R bonding orbitals **1a,b** and the lowest-lying virtual orbital 1c in accordance with our findings. Kaupp used a correction[5b,30] to the orbital energy gap of eq 3 which affords somewhat better results for PF_3 and PCl_3. The foundation of this correction is not yet clear[8a,c] and it has not been applied here.

5. General Considerations for $M(CO)_5PR_3$ Systems

It follows from Table 2 that the calculated ^{31}P chemical shifts for the phosphine substituted metal carbonyls are in good agreement with the experimental values. The theoretical estimates are derived from a single "frozen" molecule in the gas phase at 0 K without corrections for thermal motions and solvent effects. It follows further from Table 2 that it is the paramagnetic contribution to the chemical shift δ^p that determines the total value of δ in the phosphine-substituted metal carbonyls, whereas the diamagnetic δ^d term is numerically small.

TABLE 4: Paramagnetic Contributions to the Calculated ^{31}P Coordination Shift[a] in $M(CO)_5PR_3$

system	$\Delta\delta^p_{xx}$ (ppm)[c]	$\Delta\delta^p_{yy}$ (ppm)[c]	$\Delta\delta^p_{zz}$ (ppm)[c]	$\Delta\delta^b$ (exptl) (ppm)[a]
$Cr(CO)_5PH_3$	211.1	211.1	5.86	139.3 (136.5)
$Cr(CO)_5P(CH_3)_3$	118.2	118.2	2.2	85.5 (69.9)
$Cr(CO)_5PPh_3$	100.3	88.1	10.7	69.6 (63.0)
$Cr(CO)_5PF_3$	134.7	134.7	−73.0	65.4 (68.3)
$Cr(CO)_5PCl_3$	25.4	25.4	−199.9	−57.4 (−30.1)
$Mo(CO)_5PH_3$	167.0	167.0	5.6	109.0 (101.1)
$Mo(CO)_5P(CH_3)_3$	83.6	83.6	9.0	59.5 (46.4)
$Mo(CO)_5PPh_3$	82.7	65.7	11.7	55.7 (46.0)
$Mo(CO)_5PF_3$	86.7	86.7	−54.7	31.2 (41.3)
$Mo(CO)_5PCl_3$	32.5	32.5	−128.9	−28.8 (−64.7)

[a] Coordination shift: $\Delta\delta = \sigma_{PR_3} - \sigma_{[M(CO)_5PR_3]}$. [b] $\Delta\delta = \sum_{s=1}^{3}\Delta\delta^p_{ss} + \Delta\delta^d$. [c] $\Delta\delta^p_{ss} = \sigma^p_{ss,PR_3} - \sigma^p_{ss,[M(CO)_5PR_3]}$ is the difference in the paramagnetic shielding between $[M(CO)_5PR_3]$, $\sigma^p_{ss,[M(CO)_5PR_3]}$, and the ligand PR_3, σ^p_{ss,PR_3}.

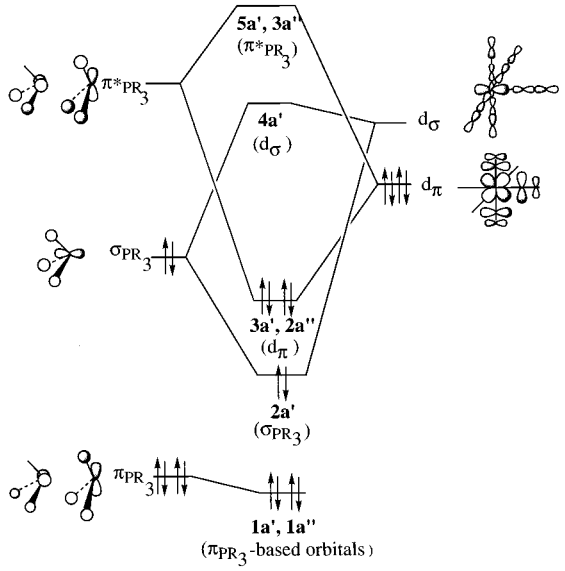

Figure 2. Schematic orbital interaction diagram for $M(CO)_5PR_3$.

Experimental shift tensor components have been reported for $Cr(CO)_5PPh_3$ and $Cr(CO)_4(CS)PPh_3$, Table 2. It is gratifying to note that the GIAO-DFT method affords δ_{ss} ($ss = xx, yy, zz$) values in reasonable agreement with experiment for these rather large systems, Table 2. We note that the δ_{xx} and δ_{yy} components perpendicular to P−M bond vector differ considerably from the corresponding δ_{xx} and δ_{yy} components of the free PPh_3 ligand perpendicular to the C_3-axis. On the other hand the δ_{zz} component along the M−P bond vector is quite similar to the δ_{zz} component along the C_3-axis in the free PPh_3 ligand. We shall now turn to an interpretation of the observed changes in the ^{31}P chemical shift as PR_3 is complexed to the metal center, $\Delta\delta$ of eq 4. The calculated and experimental values of $\Delta\delta$ for the $M(CO)_5PR_3$ systems are tabulated in Table 4. A schematic orbital interaction diagram for $M(CO)_5PR_3$ is given in Figure 2. The diagram presents the key oribtals of $M(CO)_5PR_3$ resulting from the interaction of σ_{PR_3}, π_{PR_3}, and $\pi^*_{PR_3}$ of PR_3 with d_σ and d_π of the $M(CO)_5$ fragment.

The all-dominating paramagnetic part, $\Delta\delta^p$, of the coordination shift, $\Delta\delta$, has contributions from the coupling between occupied and virtual orbitals $\Delta\delta^{oc-vir}$, as well as contributions $\Delta\delta^{oc}$ that only depend on the occupied orbitals. Our calculations show that the trends in $\Delta\delta$ between different phosphine complexes, Table 4, correlates with the paramagnetic coupling between occupied and virtual orbitals $\Delta\delta^{oc-vir}$. We have, in order to gain further insight into the coordination chemical shift,

displayed the individual components $\Delta\delta^{p}_{ss}$ ($s = x, y$, and z) of $\Delta\delta^{p}$ in Table 4.

The distortion of the PR_3 ligand on complexation has a positive contribution (<20 ppm) to $\Delta\delta^{p}_{ss}$ ($s = x, y$, and z). We have previously found[10a] that the CO bond stretch in $M(CO)_6$ has an important contribution to $\Delta\delta^{p}_{ss}$ (around 10 ppm in ^{13}C NMR and around 20 ppm in ^{17}O NMR).

6. ^{31}P Coordination Shifts in $M(CO)_5PH_3$, $M(CO)_5PMe_3$, and $M(CO)_5PPh_3$

For these systems, our calculations reveal that the two components $\Delta\delta^{p}_{xx}$ and $\Delta\delta^{p}_{yy}$ are determined principally by the paramagnetic coupling the occupied π_{PR_3}-based orbitals 1a′,-1a″ and the virtual d_σ-type orbital 4a′, Figure 2. The occupied π_{PR_3}-type orbital 1a″, **3a**, interacts with the virtual d_σ-type orbital 4a′, **3b**, through the common lobes in $\hat{M}_y|4a'\rangle$, **3c**. Similar interactions can be found for the *x*-direction involving $\hat{M}_x$.

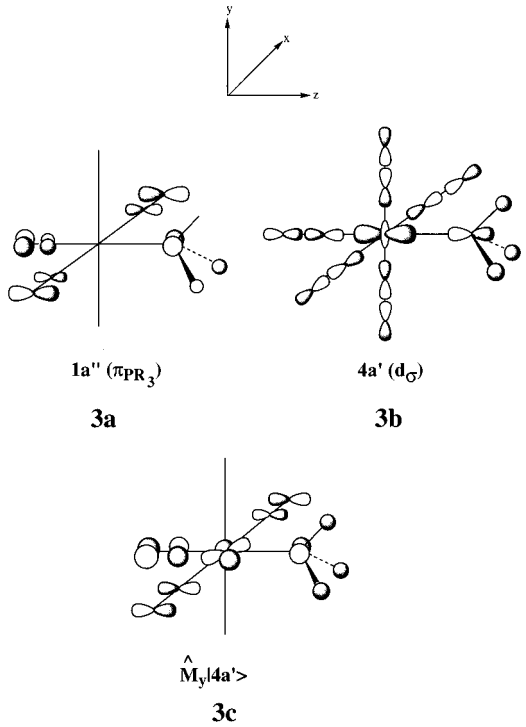

The coupling in **3c** represents a (negative) paramagnetic contribution to the ^{31}P shielding in the $M(CO)_5PR_3$ complex not present (possible) in the free PR_3 ligand. It will as a consequence afford a positive contribution to $\Delta\delta$, eq 4. The positive contribution from **3c** to $\Delta\delta$ should to a first approximation be inversely proportional to the energy gap between the 1a″ and 4a′ oribtals, eq 3. We find indeed that a decrease in the energy gap along $M(CO)_5PH_3 < M(CO)_5PMe_3 < M(CO)_5PPh_3$, Table 5, gives rise to an increase in $\Delta\delta$ following the order $M(CO)_5PH_3 > M(CO)_5PMe_3 > M(CO)_5PPh_3$ for both metals, Table 4.

We note that the energy of the virtual d_σ-type orbital 4a′, **3b**, is lower, Table 5, for $M(CO)_5PH_3$ than the energies for $M(CO)_5PMe_3$ and $M(CO)_5PPh_3$. The lower energy is in part responsible for the smaller energy gap between 1a′,1a″ and 4a′ which leads to a larger coordination shift. The low energy of 4a′, **3b**, in $M(CO)_5PH_3$ reflects the fact that PH_3 is a poor σ-donor with a σ_{PR_3} orbital of low energy, Table 3. The low energy of σ_{PH_3} will lead to a weak interaction with d_σ of $M(CO)_5$, Figure 2, and a modest destabilization of 4a′, **3b**, which is an out-of-phase combination between σ_{PH_3} and d_σ. Our analysis would indicate that the observed ^{31}P coordination shift components $\Delta\delta_{ss}$ (s = x or y) for $M(CO)_5PR_3$ and related alkyl or phenyl phosphine complexes can be taken as a measure for the degree of donation from σ_{PR_3} to d_σ with the poorest donors affording the largest values for $\Delta\delta_{ss}$ (s = x or y).

TABLE 5: Energy Gaps ΔE between 1a″ and 4a′ in $M(CO)_5PR_3$

system	energy (eV) π_{PR_3}-type 1a″	energy (eV) d_σ-type 4a′	ΔE (eV)
$Cr(CO)_5PH_3$	−10.690	−0.553	10.137
$Cr(CO)_5P(CH_3)_3$	−9.000	1.409	10.409
$Cr(CO)_5PPh_3$	−8.903	3.045	11.948
$Cr(CO)_5PF_3$	−14.766	2.163	12.603
$Cr(CO)_5PCl_3$	−12.329	−1.192	12.137
$Mo(CO)_5PH_3$	−10.696	−0.281	10.415
$Mo(CO)_5P(CH_3)_3$	−9.067	2.107	11.174
$Mo(CO)_5PPh_3$	−8.814	3.257	12.071
$Mo(CO)_5PF_3$	−14.903	−1.045	13.858
$Mo(CO)_5PCl_3$	−12.108	−0.768	11.340

TABLE 6: Population in the π^*-Type Orbitals for $M(CO)_5PR_3$ Complexes

system	total population in the two $\pi^*_{PR_3}$ orbitals
$Cr(CO)_5PH_3$	0.126
$Cr(CO)_5P(CH_3)_3$	0.120
$Cr(CO)_5PPh_3$	0.082
$Cr(CO)_5PF_3$	0.326
$Cr(CO)_5PCl_3$	0.374
$Mo(CO)_5PH_3$	0.168
$Mo(CO)_5P(CH_3)_3$	0.030
$Mo(CO)_5PPh_3$	0.064
$Mo(CO)_5PF_3$	0.260
$Mo(CO)_5PCl_3$	0.310

There is a clear reduction in the ^{31}P coordination shift for a given PR_3 ligand as we move from chromium to molybdenum, Table 4. The d_σ orbital of the 4d element forms stronger overlaps[49] with σ_{PR_3} leading to the higher energy of 4a′, Table 5, and the smaller coordination shift components $\Delta\delta_{ss}$ (s = x, y), Table 4.

The third coordination shift component $\Delta\delta_{zz}$ is very small, Table 4, for $M(CO)_5PH_3$, $M(CO)_5PMe_3$, and $M(CO)_5PPh_3$, will not be discussed any further here. We note further that the interaction between d_π of $M(CO)_5$ and $\pi^*_{PR_3}$ of the PR_3 ligand, Figure 2, is relatively weak for PH_3, $P(CH_3)_3$, and PPh_3 due to the high energy of $\pi^*_{PR_3}$, Table 3. There is as a consequence very little back-donation from d_π to $\pi^*_{PR_3}$, as illustrated in Table 6.

7. ^{31}P Coordination Shifts in $M(CO)_5PF_3$ and $M(CO)_5PCl_3$

The coordination shifts for $M(CO)_5PF_3$ and $M(CO)_5PCl_3$ are a bit more complex as already noted by Kaupp.[6f] However, we shall demonstrate that they can be interpreted as well in relatively simple terms.

The PF_3 and PCl_3 ligands have low-lying $\pi^*_{PX_3}$ orbitals, Table 3, that can interact with d_π leading to a back-donation of charge from d_π to $\pi^*_{PX_3}$ that is much larger than in the case of the PH_3, PMe_3, and PPh_3 ligands, Table 6. A result of this interaction is a destabilization of $\pi^*_{PX_3}$ as the major component in the 3a″,5a′ orbitals, Figure 2, both of which are out-of-phase combinations between d_π and $\pi^*_{PX_3}$. The back-donation will reduce the σ_{PX_3} to $\pi^*_{PX_3}$ paramagnetic couplings, **1c**, in the *x* and *y* directions and the π_{XP_3} to $\pi^*_{PX_3}$ paramagnetic coupling in the *z*-direction for the complexed PX_3 ligand compared to free PX_3 since the $\pi^*_{PX_3}$ energy effectively has been raised in

the complex as a result of the back-donation, Figure 2. The result is negative contributions to $\Delta\delta_{ss}$ ($s = x, y$) and $\Delta\delta_{zz}$. The negative contributions to $\Delta\delta_{ss}$ ($s = x, y$) and $\Delta\delta_{zz}$ are further compounded by stabilizations of σ_{PX_3} (2a′) and π_{PX_3} (1a′, 1a″) in coordinated PX_3, Figure 2, which add to the energy gap between the occupied and virtual orbitals.

It follows from Table 4 that the total coordination shift component $\Delta\delta_{zz}$ is negative and we attribute this to the above mentioned reduction of the π_{PX_3} to $\pi^*_{PX_3}$ paramagnetic coupling in the $M(CO)_5PF_3$, $M(CO)_5PCl_3$ complexes. We note in this regard that the better π-acceptor PCl_3, Table 6, has the more negative $\Delta\delta_{zz}$ component, Table 4. Our analysis would suggest that $\Delta\delta_{zz}$ in experimental studies could be used as an indicator for the degree of back-donation. The total $\Delta\delta_{ss}$ ($s = x, y$) components in Table 4 are positive as the paramagnetic coupling, **3c**, between the occupied π_{PR_3}-type orbitals 1a′,1a″, **3a**, and the virtual d_σ-type orbital 4a′, **3b**, add a positive contribution to $\Delta\delta_{ss}$ ($s = x, y$) as in the case of the PH_3, PMe_3, and PPh_3 ligands. However, it is diminished by the negative contribution from the reduction in the coupling between σ_{PX_3} and $\pi^*_{PX_3}$ for complexed PR_3. Especially PCl_3 with the strongest back-donation, Table 6, is seen to have the smallest $\Delta\delta_{ss}$ ($s = x, y$) component of all the ligands, Table 4.

The finding here that PCl_3 is a better π-acceptor than either of the other ligands considered, including PF_3, is in agreement with conclusions drawn from IR spectroscopy,[50a] metal−phosphorus NMR coupling constants,[50b] as well as M−P bond distances. There has been some discussion[15] in the literature about whether the observed ^{31}P coordination shift also support this notion. However, our analysis shows that the negative coordination shift for PCl_3 in fact is a consequence of the π-acceptor ability of this ligand.

It is well established[51] that the π-acceptor ability for CX (X = O, S, Se, and Te) increases from oxygen to tellurium. This can be explained by observing that similar overlaps between orbitals on carbon and X will decrease from X = O to X = Te. The decrease in overlap will in turn make π^*_{CX} less anti-bonding and more stable for the higher homologous. Similar arguments holds for P−X overlaps and the energy of $\pi^*_{PX_3}$ (X = F and Cl), Table 3. In fact, the π-acceptor ability should increase from X = F to X = I as $\pi^*_{PX_3}$ becomes increasingly stable. It is interesting to note that the coordination chemical shift in accordance with the arguments given above becomes increasingly negative[1] from X = F to X = I. Unfortunately, we are at the moment not able to calculate the chemical shift s of PX_3 for X = Br and I since a proper relativistic treatment including spin−orbit is required.

8. ^{95}Mo NMR

The calculated and experimental ^{95}Mo chemical shift for $Mo(CO)_5PPh_3$, $Mo(CO)_5PF_3$ and $Mo(CO)_5PCl_3$ are presented in Table 7. Our calculations clearly reproduce the observed trend in the chemical shift as $Mo(CO)_5PPh_3 < Mo(CO)_5PF_3 \ll Mo(CO)_5PCl_3$.

The trend in the ^{95}Mo chemical shift is determined by the paramagnetic shielding component σ^p with the largest contribution $\sigma^{occ-vir}$ originating from the coupling between the d_π HOMO and the d_σ LUMO, Figure 2. Both σ^p and $\sigma^{occ-vir}$, as well as the energies of d_π and d_σ, are given in Table 8.

$Mo(CO)_5PPh_3$ has the largest energy gap, 6.226 eV, and the smallest, in absolute terms, paramagnetic shielding, −2606.8 ppm. On the other hand, $Mo(CO)_5PCl_3$ presents the smallest energy gap 5.820 eV and the largest paramagnetic shielding, −3041.2 ppm, Table 8. We do not feel that the ^{95}Mo chemical shift can be used as an indication of σ-donation of π-back-donation as either type of bonding could increase the energy gap between d_π and d_σ.

TABLE 7. Calculated and Experimental ^{95}Mo Chemical Shift Tensor Components (ppm) and Isotropic Chemical Shift for Several Phosphine-Substituted Metal Carbonyls

system	δ_{xx}	δ_{yy}	δ_{zz}	δ^d	δ^p	chemical shift δ (exptl)[a]
$Mo(CO)_5PPh_3$[b]	−1668.6	−1662.1	−1837.3	4.4	−1727.1	−1722.7 (−1743.0)[c]
$Mo(CO)_5PF_3$[d]	−1760.2	−1745.4	−1753.1	6.1	−1759.0	−1752.9[e] (−1860.0)[c]
$Mo(CO)_5PCl_3$[f]	−1196.8	−1179.6	−1555.6	−2.6	−1308.0	−1310.6 (−1523.0)[c]

[a] Experimental data reported with respect to $[MoO_4]^{2-}$. [b] Reference 43. [c] Reference 15. [d] Reference 47. [e] Calculated absolute chemical shielding $\sigma_{[MoO_4]^{2-}} = -374.0$ ppm, $\sigma^d_{[MoO_4]^{2-}} = 3992$ ppm, and $\sigma^p_{[MoO_4]^{2-}} = -4366$ ppm. $\delta = \sigma_{[MoO_4]^{2-}} - \sigma_{substance}$, $\delta^d = \sigma^d_{[MoO_4]^{2-}} - \sigma^d_{substance}$, and $\delta^p = \sigma^p_{[MoO_4]^{2-}} - \sigma^p_{substance}$. [f] Optimized structure.

TABLE 8. Paramagnetic Shielding in ^{95}Mo NMR for Several Phosphine-Substituted Metal Carbonyls

system	total paramagnetic shielding σ^p (ppm)	$\sigma^{occ-vir}$ (ppm)	energy of d_π orbital (eV)	energy of d_σ orbital (eV)	energy gap (eV)
$Mo(CO)_5PPh_3$	−2638.9	−2606.8	−5.961	0.265	6.226
$Mo(CO)_5PF_3$	−2607.0	−2612.4	−7.011	−1.045	5.966
$Mo(CO)_5PCl_3$	−3057.9	−3041.4	−6.585	−0.768	5.820

9. Conclusions

We have studied the ^{31}P coordination shift $\Delta\delta$ for the phosphine-substituted metal carbonyls $M(CO)_5PR_3$ (M = Cr and Mo; $PR_3 = PH_3$, PMe_3, and PPh_3), $Cr(CO)_4CSPh_3$, and $M(CO)_5PX_3$ (X = F and Cl) as well as the ^{95}Mo NMR chemical shift in $Mo(CO)_5PPh_3$ and $Mo(CO)_5PX_3$ (X = F and Cl). This is the first theoretical NMR study on phosphine complexes that includes PPh_3 as a ligand and compares calculated and experimental shift components $\Delta\delta_{ss}$ (s = x, y, or z). Calculations on ^{95}Mo NMR for phosphine complexes have not previously been reported.

For $M(CO)_5PR_3$ (M = Cr and Mo; $PR_3 = PH_3$, PMe_3, and PPh_3) the dominating contribution, $\Delta\delta^p_{xx} + \Delta\delta^p_{yy}$, to the coordination shift comes from the paramagnetic coupling between the occupied π_{PR_3}-type orbitals and the virtual d_σ orbitals, **3c**. It is suggested that the *xx*, *yy* components of the coordination shift can be used as an indicator for the donor ability of alkyl and phenyl phosphines, with a large component corresponding to a relatively weak donor.

Our calculations indicate that PF_3 and (especially) PCl_3 are much better π-acceptors than PH_3, PMe_3, and PPh_3, in agreement with the findings from numerous previous investigations. We have shown that back-donation will reduce the σ_{PX_3} to $\pi^*_{PX_3}$ paramagnetic couplings, **1c**, in the *x*, *y* directions and the π_{PX_3} to $\pi^*_{PX_3}$ paramagnetic coupling in the *z*-direction, **2c**, for the complexed PX_3 ligand compared to free PX_3 since the $\pi^*_{PX_3}$ energy effectively has been raised in the complex as a result of the back-donation. The result is negative contributions to $\Delta\delta_{ss}$ (s = x or y) and $\Delta\delta_{zz}$ in addition to the positive contribution from **3c** to $\Delta\delta^p_{xx} + \Delta\delta^p_{yy}$. The back-donation renders the $\Delta\delta_{zz}$ component of PX_3 complexes negative and the total coordination shift for the better π-acceptor PCl_3 negative. This is the first interpretation of the complex patterns in the coordination shift of PX_3 ligands, based on quantitative calculations.

Acknowledgment. This work has been supported by the National Sciences and Engineering Research Council of Canada (NSERC). Y.R.-M. acknowledges a scholarship from DGAPA-UNAM (Mexico), and T. Z. acknowledges a Canada Council Killam Research Fellowship. We thank the Petroleum Research Fund administered by the American Chemical Society (ACS-PRF Grant 31205-AC3) for further support of this research.

References and Notes

(1) (a) Mason, J., Ed. *Multinuclear NMR*; Plenum Press: New York, 1987. (b) Fukui, H. *Magn. Reson. Rev.* **1987**, *11*, 205. (c) Chesnut, D. B. In *Annual Reports on NMR Spectroscopy*; Webb, G. A., Ed.; Academic Press: New York, 1989; Vol. 2. (d) Jameson, C. J. In *Specialist Periodic Reports on NMR*; Webb, G. A., Ed.; Royal Society of Chemistry: London, 1980−1997; Vol. 8−26. (e) Pyykkö, P. *Chem. Rev.* **1988**, *88*, 563.

(2) (a) Tossell, J. A., Ed. *Nuclear Magnetic Shiedings and Molecular Structure*; *NATO ASI Series C386*; Kluwer Academic Publishers: Dordrecht, The Netherlands. 1993. (b) Chusnut, D. B. In *Annual Reports on NMR Spectroscopy*; Webb, G. A., Ed. Academic Press: New York, 1994; Vol. 29.

(3) (a) Kutzelnigg, W.; Fleischer, U.; Schindler, M. In *NMR-Basic Principles and Progress*; Springer-Verlag: Berlin, 1990; Vol. 23, p 165. (b) Wolinski, K.; Hilton, J. F.; Pulay, P. *J. Am. Chem. Soc.* **1990**, *112*, 8251. (c) Ballard, C. C.; Hada, M.; Nakatsuji, H. *Chem. Phys. Lett.* **1995**, *254*, 170.

(4) Gauss, J.; Stanton, J. F. *J. Chem. Phys.* **1995**, *102*. 251.

(5) (a) Malkin, V. G.; Malkina, O. L.; Erikson, L. A.; Salahub, D. R. In *Modern Density Function Theory: A Tool for Chemistry*; Politzer, P.; Seminario, J. M., Eds.; Elsevier: Amsterdam, the Netherlands, 1995; Vol. 2. (b) Malkin, V. G.; Malkina, O. L.; Salahub, D. R. *Chem. Phys. Lett.* **1995**, *239*, 186. (c) Malkin, V. G.; Malkina, O. L.; Salahub, D. R. *Chem. Phys. Lett.* **1996**, *261*, 335.

(6) (a) Kaupp, M.; Malkin, V. G.; Malkina, O. L.; Salahub, D. R. *J. Am. Chem. Soc.* **1995**, *117*, 1851. (b) Kaupp, M.; Malkin, V. G.; Malkina, O. L. Salahub, D. R. *Chem. Phys. Lett.* **1995**, *235*, 382. (c) Kaupp, M.; Malkin, V. G.; Malkina, O. L.; Salahub, D. R. *Chem. Eur. J.* **1996**, *2*, 24. (d) Kaupp, M. *Chem. Eur. J.* **1996**, *2*, 348. (e) Kaupp, M. *Chem. Ber.* **1996**, *129*, 527. (f) Kaupp, M. *Chem. Ber.* **1996**, *129*, 535. (g) Kaupp, M. *J. Am. Chem. Soc.* **1996**, *118*, 3018. (h) Kaupp, M.; Malkina, O. L.; Malkin, V. G. *J. Chem. Phys.* **1997**, *106*, 9201. (i) Kaupp, M.; Malkina, O. L.; Malkin, V. G. *Chem. Phys. Lett.* **1997**, *265*, 55. (j) Kaupp, M.; Malkina, O. L.; Malkin, V. G.; Pyykkö, P. Submitted for publication.

(7) (a) Bühl, M. *Organometallics*, **1997**, *16*, 261. (b) Bühl, M. *Chem. Phys. Lett.* **1997**, *267*, 251. (c) Bühl, M. *J. Phys. Chem. A* **1997**, *101*, 2514. (d) Bühl, M.; Brintzinger H.-H.; Hopp, G. *Organometallics* **1996**, *15*, 778. (e) Bühl, M.; Malkin, V. G.; Malkina, O. L. *Helv. Chim. Acta* **1996**, *79*, 742. (f) Bühl, M. *J. Phys. Chem. A* **1997**, *101*, 2514.

(8) (a) Schreckenbach, G.; Ziegler, T. *J. Phys. Chem.* **1995**, *99*, 606. (b) Schreckenbach, G.; Dickson, R. M.; Ruiz-Morales, Y.; Ziegler, T. In *Density Functional Theory in Chemistry*; Laird, B., Ross, R., Ziegler, T., Eds.; American Chemical Society: Washington, DC, 1996; p 328. (c) Rauhut, G.; Puyear, S.; Wolinski, K.; Pulay, P. *J. Phys. Chem.* **1996**, *100*, 6103. (d) Cheeseman, J. R.; Trucks, G. W.; Keith, T. A.; Frisch, M. J. *J. Chem. Phys. 104*, 5497. (e) Lee, A. M. Handy, N. C.; Colwell, S. M. *J. Chem. Phys.* **1995**, *103*, 10095.

(9) (a) London, F. *J. Phys. Radium* **1937**, *8*, 397. (b) Ditchfield, R. *Mol. Phys.* **1974**, *27*, 789. (c) Bieger, W.; Seifert, G.; Eschrig, H.; Grossmann, G. *Chem. Phys. Lett.* **1985**, *115*, 275. (d) Friedrich, K.; Seifert, G.; Grossmann, G. *Z. Phys.* **1990**, *D17*, 45.

(10) (a) Ruiz-Morales, Y.; Schreckenbach, G.; Ziegler, T. *J. Phys. Chem.* **1996**, *100*, 3359. (b) Ruiz-Morales, Y.; Schreckenbach, G.; Ziegler, T. *Organometallics* **1996**, *15*, 3920. (c) Ruiz-Morales, Y.; Schreckenbach, G.; Ziegler, T. *J. Phys. Chem.* **1997**, *101*. 4121. (d) Schreckenbach, G.; Ruiz-Morales, Y.; Ziegler, T. *J. Chem. Phys.* **1996**, *104*, 8605. (e) Ehlers, A. W.; Ruiz-Morales, Y.; Baerends, E. J.; Ziegler, T. *Inorg. Chem.* **1997**, *36*, 5031−5036.

(11) (a) Schreckenbach, G.; Ziegler, T. *Int. J. Quantum Chem.* **1996**, *60*, 753. (b) Schreckenbach, G.; Ziegler, T. *Int. J. Quantum Chem.* **1997**, *61*, 899.

(12) (a) Godbout, N.; Oldfield, E. *J. Am. Chem. Soc.* **1997**, *119*, 8065. (b) Becke, A. D. *J. Chem. Phys.* **1993**, *98*, 5648.

(13) (a) Nakatsuji, H.; Takashima, H.; Hada, M. *Chem. Phys. Lett.* **1995**, *233*, 95. (b) Nakatsuji, H.; Nakajima, T.; Hada, M.; Takashima, H.; Tanaka, S. *Chem. Phys. Lett.* **1995**, *247*, 418. (c) Nakatsuji, H.; Hada, M.; Tejima, T.; Nakajima, T.; Sugimoto, M. *Chem. Phys. Lett.* **1995**, *249*, 284.

(14) (a) Wasylishen, R. E.; Eichele, K.; Nelson, J. H. *Inorg. Chem.* **1996**, *35*, 3905. (b) Power, P. W.; Wasylishen, R. E.; Curtis, R. *Can. J. Chem.* **1989**, *67*, 454. (c) Eichele, K.; Wasylishen, R. E.; Britten, J. F. *Inorg. Chem.* **1997**, *36*, 3539. (d) Eichele, K.; Wasylishen, R. E.; Nelson, J. H. *J. Phys. Chem.* **1997**, *101*, 5463. (e) Malito, J. *Annu. Rep. NMR Spectrosc.* **1997**, *33*, 151.

(15) (a) Song, S.; Alyea, E. C. *Can. J. Chem.* **1996**, *74*, 2304. (b) Alyea, E. C.; Song, S. *Inorg. Chem.* **1995**, *34*, 3864.

(16) Baerends, E. J.; Ellis, D. E.; Ros, P. *Chem. Phys.* **1973**, *2*, 41.

(17) Baerends, E. J.; Ros, P. *Chem. Phys.* **1973**, *2*, 52.

(18) Baerends, E. J. PhD Thesis, Free University, Amsterdam, The Netherlands, 1973.

(19) Baerends, E. J.; Ross, P. *Int. J. Quantum Chem. Symp.* **1978**, *12*, 169.

(20) te Velde, G.; Baerends, E. J. *Int. J. Quantum Chem.* **1988**, *33*, 87.

(21) te Velde, G. *Amsterdam Density Functional (ADF), User Guide*, Release 1.1.3; Department of Theoretical Chemistry, Free University: Amsterdam, The Netherlands, 1994.

(22) Becke, A. *Phys. Rev.* **1988**, *A38*, 3098.

(23) Perdew, J. *Phys. Rev.* **1986**, *B33*, 8822.

(24) Vernoijs, P.; Snijders, J. G.; Baerends, E. J. *Slater Type Basis Functions for the Whole Periodic System*; Internal report (in Dutch); Department of Theoretical Chemistry, Free University: Amsterdam, The Netherlands, 1981.

(25) Snijders, J. G.; Baerends, E. J.; Vernoijs, P. *At. Nucl. Data Tables* **1982**, *26*, 483.

(26) Krijn, J.; Baerends, E. J. *Fit Functions in the HFS Method*; Internal Report (in Dutch); Department of Theoretical Chemistry, Free University: Amsterdam, The Netherlands, 1984.

(27) Ballhausen, C. J. In *Introduction to Ligand Field Theory*; McGraw-Hill: New York, 1962; pp 149.

(28) McGlynn, S. P.; Vanquickenborn, L. G.; Kinoshita, M.; Carroll, D. G. In *Introduction to Applied Quantum Chemistry*; Holt, Rinehart and Winston: New York, 1972.

(29) (a) Pople, J. A.; Schneider, W. G.; Bernstein, H. J. *High-Resolution Nuclear Magnetic Resonance*; McGraw-Hill: New York, 1959. (b) Elschenbroich, C.; Salzer, A. *Organometallics. A Concise Introduction*; Verlag Chemie: Weinheim, Germany, 1992.

(30) Bouman, T. D.; Hansen, A. E. *Chem. Phys. Lett.* **1990**, *175*, 292.

(31) The bracket notation $\langle\Psi_1|\hat{M}_s|\Psi_2\rangle$ denotes certain matrix elements (integrals) between the two orbitals Ψ_1 and Ψ_2 that contribute to the paramagnetic shielding σ^p.

(32) The expression $|\hat{M}_x|\pi^*_{PR_3}\rangle$ denotes an orbital resulting from the action of the operator $\hat{M}_x$ on the $\pi^*_{PR_3}$ orbital.

(33) Pregosin, P. S.; Kunz, R. W. *NMR Basic Principles and Progress*; Diehl, P., Fluck, E., Kosfeld, R., Eds.; Springer-Verlag: New York, 1979.

(34) Masse, R.; Tordjman, I. *Acta Crystallogr. C: Cryst. Struct. Commun.* **1990**, *46*, 606.

(35) Moser, E.; Fischer, E. O.; Bathelt, W.; Gretner, W.; Knauss, L.; Louis, E. *J. Organomet. Chem.* **1969**, *19*, 337.

(36) Bruckmann, J.; Kruger, C. *Acta Crystallogr. C: Cryst. Struct. Commun.* **1995**, *51*, 1155.

(37) Greenwood, N. N.; Earnshaw, A. *Chemistry of the Elements*; Pergamon Press; NY, 1994; pp 564, 568.

(38) Lee, K. J.; Brown, T. L. *Inorg. Chem.* **1992**, *31*, 289.

(39) Mathieu, R.; Lenzi, M.; Poilblanc, R. *Inorg. Chem.* **1970**, *9*, 2030.

(40) Huang, Y.; Uhm, H. L.; Gilson, D. F. R.; Butler, I. S. *Inorg. Chem.* **1997**, *36*, 435.

(41) Chekhlov, A. N. *Kristallografiya* **1993**, *18*, 79.

(42) Plastas, H. J.; Stewart, J. M.; Grim, S. O. *Inorg. Chem.* **1973**, *12*, 265.

(43) Davies, M. S.; Aroney, M. J.; Buys, I. E.; Hambley, T. W.; Calvert, J. L. *Inorg. Chem.* **1995**, *34*, 330.

(44) Cotton, F. A.; Darensbourg, D. J.; Ilsley, W. H. *Inorg. Chem.* **1981**, *20*, 578.

(45) Jameson, C. J.; De Dios, A.; Jameson, A. K. *Chem. Phys. Lett.* **1990**, *167*, 575.

(46) Macintyre, J. E., Ed. *Dictionary on Inorganic Compounds*; Chapman and Hall: Cambridge, Great Britain, 1992; p 2932.

(47) Bridges, D. M.; Holywell, G. C.; Rankin, D. W. *J. Organomet. Chem.* **1971**, *32*, 87.

(48) Dove, M. F. A.; Jones, E. M. L.; Clark, R. *J. Magn. Reson. Chem.* **1989**, *27*, 973.

(49) Ziegler, T.; Tschinke, V.; Ursenbach, C. *J. Am. Chem. Soc.* **1987**, *109*, 4827. (b) Li, J.; Schreckenbach, G.; Ziegler, T. *J. Am. Chem. Soc.* **1995**, *117*, 486.

(50) (a) Graham, W. A. G. *Inorg. Chem.* **1968**, *7*, 315. (b) Masters, A. F.; Brownlee, R. T. C.; O'Connor, M. J.; Wedd, A. G. *J. Organomet. Chem.* **1985**, *290*, 365.

(51) Ziegler, T. *Inorg. Chem.* **1985**, *25*, 2721.